N89-24916

COMPUTER SIMULATIONS OF COSMIC-RAY DIFFUSION NEAR SUPERNOVA REMNANT SHOCK WAVES

C E Max
Institute of Geophysics and Planetary Physics, Lawrence Livermore National Laboratory

A L Zachary
Dept. of Astronomy & Astrophysics, University of Chicago

J Arons
Lawrence Livermore National Laboratory & University of California at Berkeley+*

ABSTRACT

We have used a new plasma simulation model to study the resonant interactions between streaming cosmic-ray ions and a self-consistent spectrum of Alfven waves, such as might exist in the interstellar medium upstream of a supernova remnant shock wave. The computational model is a hybrid one, in which the background interstellar medium is an MHD fluid and the cosmic-rays are discrete kinetic particles. The particle sources for the electromagnetic fields are obtained by averaging over the fast cyclotron motions. When the perturbed magnetic field is larger than about 10% of the background field, the macro- and micro-physics are no longer correctly predicted by quasi-linear theory. The particles are trapped by the waves and show sharp jumps in their pitch-angles relative to the background magnetic field, and the effective ninety-degree scattering time for diffusion parallel to the background magnetic field is reduced to between 5 and 30 cyclotron periods. We use our simulation results to suggest that Type I supernova remnants may be the principal sites of cosmic ray acceleration.

Keywords: cosmic-ray acceleration, first-order Fermi acceleration, shock acceleration, upstream waves, quasilinear diffusion, supernova remnants

1. INTRODUCTION

In the late 1970's, several authors almost simultaneously suggested that cosmic-rays can be accelerated by a first-order Fermi mechanism, brought about as they scatter many times across astrophysical shock waves (Ref. 1). In the context of explaining the energy density and spectrum of galactic cosmic rays, the shock waves driven by expanding supernova remnants give the most likely setting for such acceleration. This hypothesis is attractive for at least two reasons: 1) it predicts a power-law particle spectrum similar to that deduced as the source spectrum for galactic cosmic rays, and 2) the overall energetics of galactic supernovae is sufficient to account for the observed cosmic-ray energy density, provided that the acceleration process is at least a few percent efficient.

However the fact that the cosmic-ray source spectrum seems to extend smoothly up to 10^{14} - 10^{15} eV poses a potential difficulty for these theories. The reason is as follows. In diffusive cosmic-ray acceleration, a particle gains a small amount of energy each time it is scattered across the shock front. The highest-energy particles must cross and re-cross the shock front many times in the process of being accelerated. Thus considerable amounts of time are required to accelerate the highest-energy cosmic-rays.

The effective upper limit on the energy to which a particle can be accelerated in these first-order Fermi-acceleration theories is given by equating the acceleration time to an estimate of the lifetime of the supernova remnant (Ref. 2). Using a minimum value of the spatial diffusion coefficient

$$D_{min} = r_L v / 3, \qquad (1)$$

where r_L is the ion Larmor radius based on the background field, Lagage and Cesarsky[2] obtained an upper limit on the cosmic-ray energy:

$$E_{max} < \text{a few} \times 10^{13} (B_0 / 10^{-6} \text{ gauss}) Z/A \text{ eV}. \qquad (2)$$

Here Z/A is the nuclear charge-to-mass ratio of the cosmic-ray ion and B_0 is the value of the interstellar magnetic field. This result is puzzling, since the cosmic-ray source spectrum is observed to be smooth in slope and continuous in value to energies in excess of this limit, suggesting that there is not a transition in acceleration mechanisms at the energy given by equation (2). One would like to establish a more realistic maximum cosmic-ray energy by using a self-consistently derived diffusion coefficient to replace that in Eqn. (1). The computational simulations we describe here can begin to address this issue by explicitly evaluating the diffusion coefficient of fast particles in a self-consistent spectrum of Alfven waves, and studying its scaling with cosmic-ray flux.

Proceedings of the Joint Varenna-Abastumani International School & Workshop on Plasma Astrophysics, held in Varenna, Italy, 24 Aug.–3 Sept. 1988 (ESA SP-285, Vol. I, Dec. 1988).

The efficiency of diffusive cosmic-ray acceleration is also an important issue. First-order Fermi acceleration predicts that the efficiency depends on the spatial diffusion coefficient, which itself depends on the scattering rate. Frequently, quasi-linear assumptions have been used to describe scattering in the self-consistent spectrum of Alfven waves upstream of the shock front. Yet several different arguments (Ref. 3) suggest that the Alfven-wave perturbations near the shock are large ($\delta B/B_0 > 1$), thus violating the initial quasi-linear assumptions. Recent observations of fast particles and Alfven waves at interplanetary shocks (Ref. 4) show several types of non-quasi-linear behavior. The computer simulation study described here allows a more general examination of these effects, since it does not require quasi-linear conditions to be satisfied.

2. THE COMPUTATIONAL MODEL

The intention is to model a region upstream of a supernova remnant shock-wave, in which there exists an anisotropic distribution of cosmic-rays as a consequence of the previous action of the shock-acceleration process. The shock-wave itself is not included in the simulation volume; its presence is reflected via the anisotropy of the initial cosmic-ray distribution. We study the time evolution of this initially anisotropic cosmic-ray distribution, together with the self-consistent Alfven waves which it produces.

Our simulation model is an orbit-averaged Darwin quasi-neutral hybrid code (Ref. 5). In less technical terms, this means the following. The electrons and ions in the interstellar medium are treated as a single ideal MHD (magnetohydrodynamic) fluid, while the cosmic-ray ions are treated as discrete kinetic particles. The displacement current is assumed small relative to plasma currents, and the cosmic-ray number density is assumed small relative to the density of the interstellar medium.

The simulation geometry is one-dimensional, with a periodic grid having either 128 or 256 mesh points. Magnetic and electric fields are defined on the grid points. The direction of spatial variation (the x-axis) is parallel to the background magnetic field, so that all waves propagate parallel or antiparallel to $\mathbf{B}_0$. All perturbed magnetic fields are perpendicular to the background field.

Cosmic-rays are represented by 32000 discrete particles, whose currents contribute as sources for the self-consistent magnetic and electric fields at the grid points. Particle positions are defined along the whole x-axis, not just at grid points. Particle trajectories in position and velocity are integrated via micro-timesteps Δt, with resolution sufficient to follow the cyclotron motion in detail. Currents due to the particles are averaged over much larger time intervals ΔT, where typically $N = \Delta T/\Delta t = 88$. This orbit-averaging method allows the field-solve to be done much less frequently than the particle-push. In addition, it results in a discrete-particle noise level that is lower by a factor of N than that which would otherwise obtain for the same number of cosmic-ray particles in the absence of orbit-averaging (Ref. 6). As a consequence, it is practical to simulate instabilities

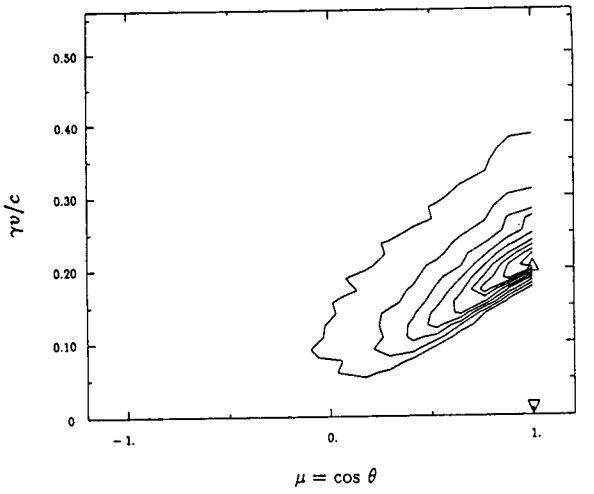

Figure 1: Initial cosmic-ray distribution function for Models A and B. Contours show equal values of $p^2 f(p)$; vertical axis is $p/mc = \gamma v/c$; horizontal axis is the cosine of the particle's pitch-angle relative to $\mathbf{B}_0$.

which grow slowly relative to the cyclotron period of the cosmic-rays.

The initial distribution function of the cosmic-rays is a power-law in the magnitude of the momentum, with spectral index 4:

$$f(p)\, d^3p \propto p^{-4}\, d^3p\,, \quad 0.1 \le \gamma v/c \le 2.0\,. \qquad (3)$$

This power-law momentum distribution is then taken to be drifting relative to the laboratory frame with a (non-relativistic) drift velocity $v_D = 0.1\ c = 10\ v_A$, where v_A is the Alfven speed:

$$v_A^2 = B_0^2 / 4\,\pi\,\rho\,. \qquad (4)$$

Figure 1 illustrates the initial shape of this drifting power-law cosmic-ray distribution function in our simulations.

We shall discuss in some detail two contrasting simulations, Model A and Model B, which differ only in the initial density of cosmic-rays relative to the background interstellar medium:

$$\text{Model A: } n_{cr}/n_{ism} = 4 \times 10^{-3}\,;\ n_{cr} v_D / n_{ism} v_A = 0.04\,;$$

$$\text{Model B: } n_{cr}/n_{ism} = 4 \times 10^{-2}\,;\ n_{cr} v_D / n_{ism} v_A = 0.40 \qquad (5)$$

3. RESULTS OF THE SIMULATIONS

The overall evolution in both Model A and Model B is as follows. The initial anisotropy of the cosmic-rays relative to $\mathbf{B}_0$ drives a resonant Alfven-wave instability in the interstellar medium. A broad spectrum of Alfven waves grows up in time, since modes with different wavenumbers k can resonate with different particles in the power-law distribution function. When the Alfven waves reach large amplitude, mode-coupling between them also drives sound-wave fluctuations in the

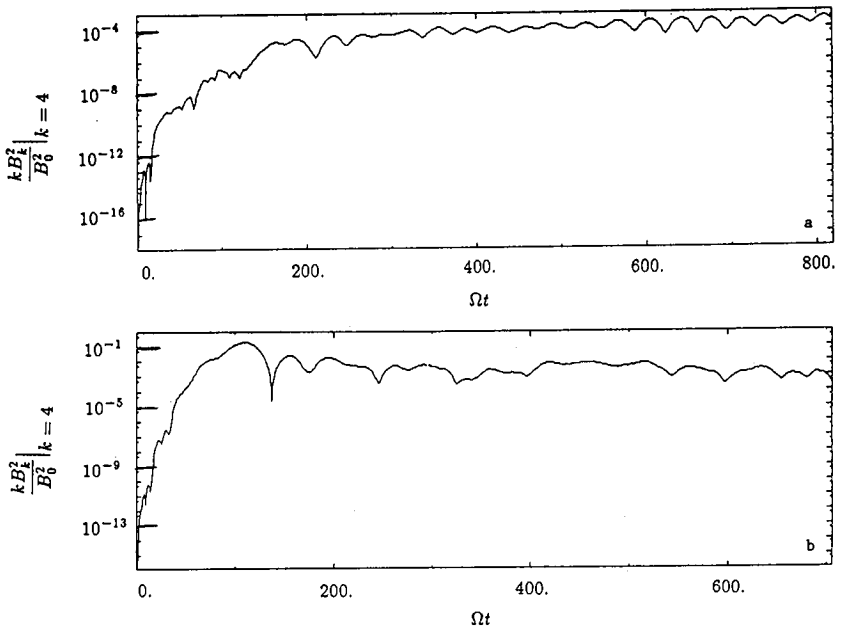

Figure 2: Time histories of energy density in the most unstable Alfven-wave mode. a) Model A, $n_{cr}/n_{ism} = 4 \times 10^{-3}$; b) Model B, $n_{cr}/n_{ism} = 4 \times 10^{-2}$. Vertical axis is kB_k^2/B_0^2, horizontal axis is cyclotron frequency times time.

background interstellar medium. As a consequence of the Alfven-wave fluctuations, the mean cosmic-ray drift velocity decreases from its initial level as individual cosmic-rays are scattered in pitch-angle.

Frames a and b of Figure 2 show the time evolution of energy in the largest unstable Alfven-wave mode for Models A and B respectively. An initial period of exponential growth of the resonant anisotropy-driven instability is followed by saturation of the Alfven-wave amplitudes. For Model A (the low-flux case), root-mean-square magnetic field perturbations in the saturated phase are $(\delta B/B_0)_{rms} \simeq 3 \times 10^{-2}$; individual magnetic-field peaks with amplitudes $(\delta B/B_0)_{peak} \simeq 0.15$ are present in snapshots of $\delta B/B_0$ as a function of x. For Model B (the high-flux case), rms magnetic field perturbations in the saturated phase are $(\delta B/B_0)_{rms} \simeq 0.2 - 0.3$, with individual peak field amplitudes $(\delta B/B_0)_{peak} \simeq 0.9 - 1.1$. Thus one interesting lesson is that the description of a spectrum of Alfven-waves in terms of rms perturbation levels can lead one to forget that individual magnetic-field maxima are present at values many times larger than the rms level. We shall see below that these larger-than-average peaks can have a strong influence on the non-quasilinear behavior of the particle scattering.

For Model A, the low-flux simulation, the Alfven-waves propagate forward (in the direction of the cosmic-ray anisotropy). However for Model B, where the Alfven-wave amplitudes are larger, we observe some backward propagating Alfven-waves. We also observe sound-wave perturbations in the background interstellar medium, driven by wave-wave coupling between different Alfven wave modes. We have suggested elsewhere (Ref. 7) that sound-waves driven by Alfven-wave turbulence upstream of astrophysical shocks may contribute to the electron density fluctuations inferred from interstellar scintillation measurements. Figure 3 illustrates the Alfven-wave amplitudes (left panel) and the sound-wave amplitudes (right panel) as functions of x and t, for Model B. Forward propagation corresponds to a line moving upwards and to the right in these pictures.

As a result of scattering of individual cosmic-rays by the Alfven waves, the mean drift velocity v_D of the cosmic-

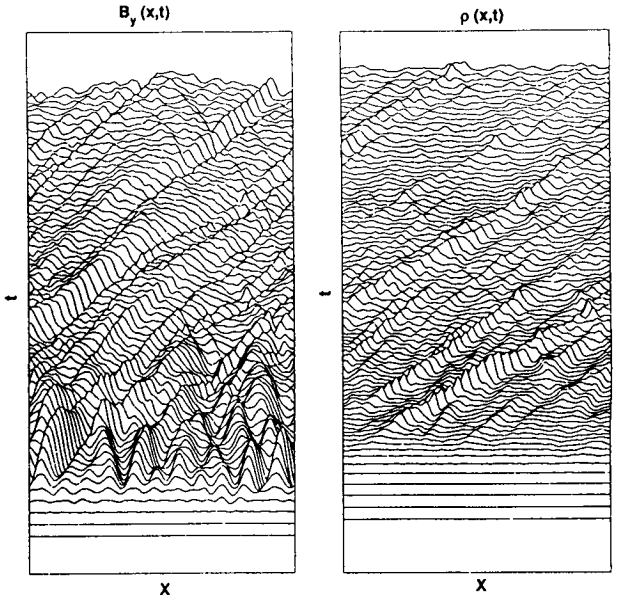

Figure 3: Amplitudes of Alfven waves (left panel) and sound waves (right panel) in Model B, as functions of x and t.

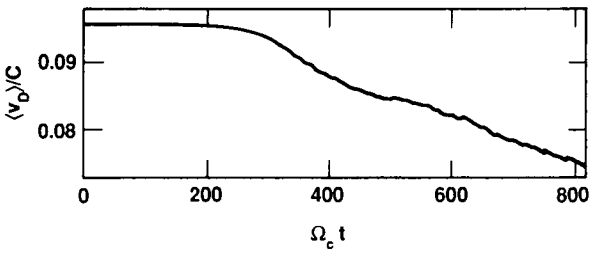

Figure 4: Time evolution of cosmic-ray drift velocity, v_D , in Model A. Horizontal axis is cyclotron frequency times the time.

rays decreases with time. Figure 4 shows the decline of v_D/c with time for Model A, the low-flux simulation. The horizontal axis $\Omega_c t$ is the cyclotron frequency times the time.

We have used test-particles to study the scattering process of cosmic-rays in these self-consistent Alfven-wave spectra. In frames a and b of Figure 5, we plot the trajectories of two typical test-particles in Models A and B respectively. The vertical axis μ in these plots is the cosine of the particle's pitch-angle relative to the actual magnetic field; the horizontal axis Ωt is the cyclotron frequency times the time. We have constructed analogous trajectory plots using the pitch-angle relative to the background magnetic field B_0 , which is more relevant to calculation of the spatial diffusion coefficient; we find similar results to those shown here.

The test-particle in Model A, the low-flux case, shows a trajectory that is qualitatively diffusive in nature, made up of a sequence of small changes in pitch-angle. This is the type of behavior that is predicted by quasi-linear theory. Note, however, that the particle diffuses through $\mu = 0$ without any hesitation, whereas lowest-order quasilinear theory predicts that diffusion through $\mu = 0$ should not be possible.

The test-particle in Model B, the high-flux case, shows markedly different behavior. Its trajectory is dominated by large jumps in pitch-angle, $\delta\mu/\mu \approx 1$, within 5 to 10 cyclotron periods, and by repeated passes through $\mu = 0$. These large jumps in pitch-angle are decidedly non-quasilinear, since they involve order-unity changes in pitch-angle in a few cyclotron periods. To investigate their physical origin, we followed in detail all of the forces experienced by a test-particle during one jump from $\mu \approx +1$ to $\mu \approx -1$. The largest systematic force is the x-component of the Lorentz force, $(\delta v_\perp \times \delta B_\perp)_x$, representing the nonlinear force due to the perturbed particle velocity and the perturbed magnetic field.

Figure 6 shows the time evolution of this $(\delta v_\perp \times \delta B_\perp)_x$ force on the test-particle during its rapid jump from $\mu \approx +1$ to $\mu \approx -1$. Note that the timescale on the horizontal axis is greatly expanded relative to that in Figure 5. During the rapid jump, the particle experiences a series of brief intervals when the $(\delta v_\perp \times \delta B_\perp)_x$ force is large, both in the positive and negative directions. However during this particular time interval there are four large negative spikes in $(\delta v_\perp \times \delta B_\perp)_x$ which outweigh the smaller positive spikes, and which together are responsible for the large net force on the test particle in the negative x direction. One interpretation of these large negative spikes is that they represent intervals during which the test-particle experiences magnetic trapping in large-amplitude Alfven waves. This is supported by the analysis in Ref. 6 of the phase angle ψ

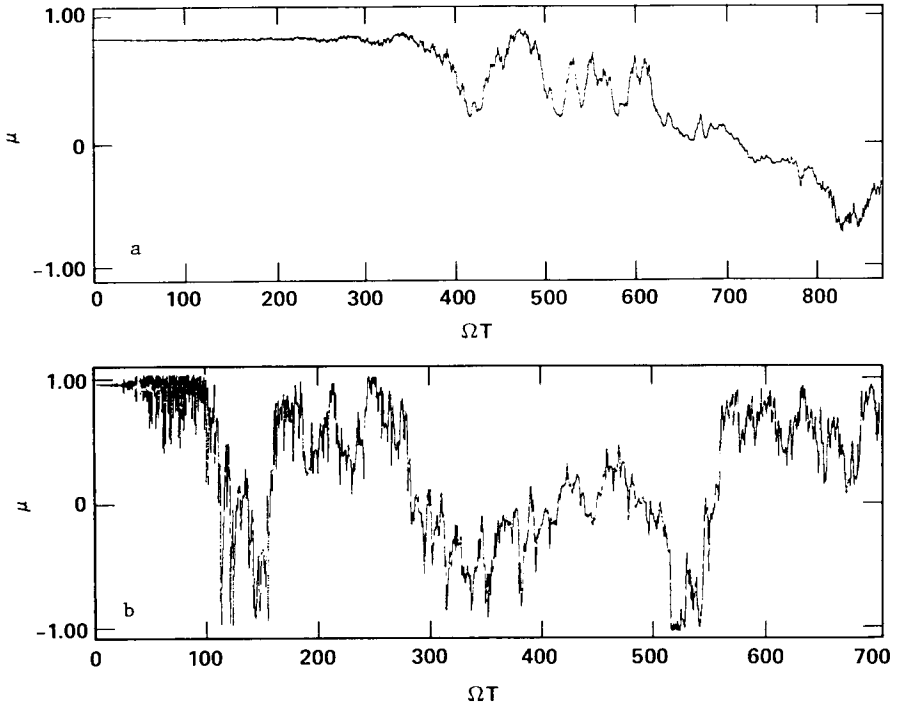

Figure 5: Trajectories of test particles showing evolution of pitch-angle $\mu = \cos\theta$, as function of the cyclotron frequency times the time. a) Test particle in Model A (low cosmic-ray flux); b) The same test particle in Model B (high cosmic-ray flux).

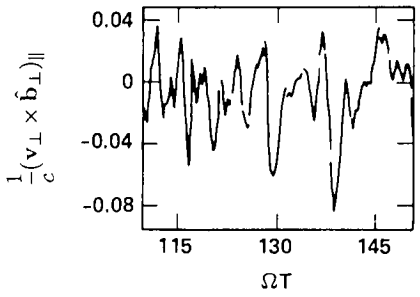

Figure 6: The x-component of the $\mathbf{v} \times \mathbf{B}$ force on a test particle in Model B, during the brief time interval when the particle is undergoing a sharp negative jump in pitch-angle. Vertical axis is x-component of the Lorentz force, normalized to B_0 ; horizontal axis is cyclotron frequency times the time, using a greatly expanded scale.

between $v_\perp$ and $B_\perp$, which pauses near zero degrees during the main negative spikes shown in Figure 6.

We conclude from these results that the higher-flux simulation, Model B, shows substantial non-quasilinear behavior, particularly in its particle scattering characteristics. To assess the effect on the spatial diffusion coefficient of cosmic-rays, we have computed the effective ninety-degree scattering time in our simulations using an ensemble of test-particles. We compute the ninety-degree scattering time as a function of the magnitude of the particle momentum, for each of the simulation conditions we have modeled. The calculation is based on constructing the auto-correlation function of the pitch-angle relative to B_0, followed along a test-particle's trajectory:

$$C_\mu(\tau) = (1/T_{max}) \int_0^{T_{max}} (\mu(t) - <\mu>)(\mu(t+\tau) - <\mu>)\, dt \quad (6)$$

The autocorrelation time τ_{ac} is calculated from the half-width of the central peak of $C_\mu(\tau)$. The ninety-degree scattering time τ_{90} is then given by

$$\tau_{90} \simeq < \tau_{ac} / C_\mu(\tau = 0) > , \quad (7)$$

where the brackets indicate an ensemble average over all of the test-particles. Further details of this calculation, as well as graphs showing the autocorrelation functions themselves, may be found in Ref. 6.

4. IMPLICATIONS FOR COSMIC-RAY ACCELERATION

4.1 Scaling Laws

Computational realities have constrained us to simulate only a relatively small portion of the parameter space of interest to cosmic-ray acceleration at supernova remnant shock-waves. Thus, for example, our results do not apply directly to the scattering of the highest-energy cosmic-rays, since the simulations lack sufficient dynamic range in particle energy. However, we can use our simulation results to construct scaling laws and upper limits for the important physical quantities involved in diffusive acceleration. These scaling-laws give a suggestion of the physical behavior that will apply for parameter ranges which are presently out of reach of direct computational simulation.

In particular, the values of the ninety degree scattering time constructed from our simulations can be used to investigate the scaling of the cosmic-ray diffusion coefficient. The spatial diffusion coefficient is given by

$$D \simeq v^2 \tau_{90} / 3 ; \quad (8)$$

we can use the values of τ_{90} from our simulations to investigate D . First we consider the variation of τ_{90} with the amplitude of the magnetic-field perturbations. Figure 7 shows the dependence of the cyclotron frequency times the ninety degree scattering time, $\Omega\tau_{90}$, on the root-mean-square strength of the magnetic field perturbations, denoted here by $\delta B/B_0$. The three curves shown in Figure 7 correspond to three different values of the magnitude of the particle momentum, $\gamma v/c$. An approximate fit to these curves is given by the following relations:

$$\Omega\tau_{90} \approx K_1 (\delta B/B_0)^{-3 \pm 0.6}, \quad 0.4 \leq \delta B/B_0 \leq 0.7 ;$$

$$\Omega\tau_{90} \approx K_2 (\delta B/B_0)^{-0.4}, \quad 0.06 \leq \delta B/B_0 \leq 0.4 ; \quad (9)$$

where $K_1 \simeq 1.1 \times 10^{1 \pm 0.2}$, and $K_2 \simeq 140$.

Recall that the quasi-linear model normally used for calculations of cosmic-ray scattering is that of Jokipii (Ref. 8), which predicts that

$$\Omega\tau_{90} \simeq (4/\pi)\,(B_0^2/kB_k^2), \quad (10)$$

where B_k is the Fourier amplitude of the magnetic field

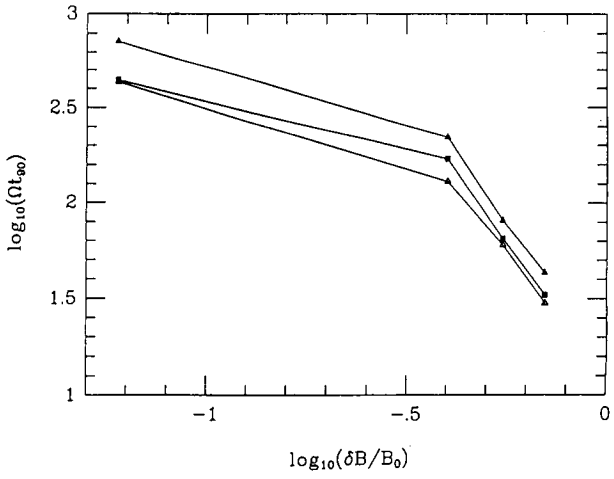

Figure 7: Scaling relation between ninety degree scattering time τ_{90} and root-mean-square amplitude of magnetic field perturbations $\delta B/B_0$, from a collection of simulations. Lines represent ninety-degree scattering for different particle momenta: p/mc = 0.1 (filled triangles), 0.2 (filled squares), and 0.4 (empty triangles).

fluctuations at wavenumber k. If we roughly equate kB_k^2/B_0^2 in Eqn. (10) with $(\delta B/B_0)^2$, then Jokipii's quasilinear theory would predict $\Omega r_{90} \propto (\delta B/B_0)^{-2}$ in Eqn. (9), which should apply at the lower values of $\delta B/B_0$. Instead, the observed dependence $\Omega r_{90} \propto (\delta B/B_0)^{-0.4}$ for small values of $\delta B/B_0$ is considerably weaker than this prediction. We conclude that for the perturbation amplitudes we have studied ($\delta B/B_0 \geq 0.06$) , the ninety-degree scattering times seen in our simulations do not follow the simple quasilinear trends generally assumed in theories of cosmic-ray diffusion.

4.2 Maximum Energy of Cosmic-Rays

As a substitute for quasi-linear theory, we can use the empirical relations given in Eqn. (9) and Figure 7 to calculate E_{max} , the maximum cosmic-ray energy that can be produced during the active lifetime of a supernova remnant. We shall follow the general approach of Lagage and Cesarsky (Ref. 2), using our empirically derived scaling for the ninety degree scattering time. We calculate the cosmic-ray momentum as a function of time, using the Sedov solution for the evolution of the supernova remnant shock-wave, and find the asymptotic maximum cosmic-ray energy E_{max} together with the time needed to achieve this energy.

Since we are not able to simulate directly the scattering of particles with energies typical of the highest-energy cosmic rays (10^{14} - 10^{15} eV), we shall have to make some assumptions concerning the self-consistent behavior of these particles and of the Alfven waves which scatter them. According to resonant quasi-linear theory, particles at a given momentum p generate the waves by which they are themselves scattered, at the resonant wavenumber $k(p) = 1 / r_L(p) \propto \gamma^{-1}$. The highest-energy cosmic-rays are rare compared with those at lower energies, because of the power-law distribution function (Eqn. 3). As a result, one might expect the wave amplitudes at small k (long wavelength) to be smaller than those at higher k. To derive an upper limit for E_{max} , we neglect this wavelength distinction and assume that the scaling results of our simulations also apply to particles having higher energies than those present in the simulations.

Assuming a spatially uniform diffusion coefficient, Lagage and Cesarsky found the rate of gain of momentum for a particle encountering a shock in a diffusive manner to be

$$p^{-1}\, dp/dt = (u_1 - u_2)(u_1 u_2)/[3D (u_1 + u_2)] \qquad (11)$$

where u_1 and u_2 are the fluid velocities up and downstream of the shock, measured in the shock frame. We assume a strong shock, so that $u_2/u_1 = 1/4$. If we substitute our results from Eqn. (9) into Eqn. (8) for D, and then use this diffusion coefficient in Eqn. (11), we find for relativistic particles that

$$dp/dt = (3/20) (eB_0 / \Omega r_{90}) (u_1 / c)^2$$
$$= (3eB_0/20K_{1,2})(\delta B/B_0)^{\alpha} (u_1/c)^2 \qquad (12)$$

where K_1 and K_2 are defined below Eqn. (9) and

$$\alpha = 3 \pm 0.6 , \quad 0.4 \leq \delta B/B_0 \leq 0.7 ,$$
$$\alpha = 0.4 , \quad 0.06 \leq \delta B/B_0 \leq 0.4 . \qquad (13)$$

Here B_0 is the magnitude of the background magnetic field upstream of the shock.

We evaluate u_1 in Eqn. (12) using the Sedov solution for the expansion history of the supernova remnant. This means we assume in this discussion that the cosmic-ray pressure is less than the ram pressure at the shock front, so that the shock speed is not strongly modified by the presence of the cosmic rays. If we normalize to parameters typical of Type II galactic supernovae and of a hot Phase III interstellar medium, then the upstream velocity in the shock frame is

$$u_1 \approx (10^{3.5} \text{ km s}^{-1}) \times (v_{ej}/10^{3.5} \text{ km s}^{-1}) (t/t_1)^{-3/5} \qquad (14)$$

where v_{ej} is the initial ejecta expansion velocity and t_1 is the time for the ejecta to sweep up their own mass from the interstellar medium:

$$t_1 \approx (10^{3.5} \text{ years})(E_{SN}/10^{51} \text{ ergs})^{1/3} (n_{ism}/10^{-2} \text{ cm}^{-3})^{-1/3}$$
$$\times (v_{ej}/10^{3.5} \text{ km s}^{-1})^{-5/3} . \qquad (15)$$

Substituting expression (14) for u_1 into Eqn. (12), we can integrate to find the time dependence of the cosmic-ray momentum:

$$p(t) = p_{\infty} [1 - (0.91\, t_1 / t)^{1/5}] \qquad (16)$$

where

$$p_{\infty} \approx (7 \times 10^{12} \text{ eV/c}) \times (B_0/10^{-6} \text{ gauss}) (11Z/AK_{1,2})$$
$$\times (\delta B/B_0)^{\alpha} (E_{SN}/10^{51} \text{ ergs})^{1/3} (n_{ism}/10^{-2} \text{ cm}^{-3})^{-1/3}$$
$$\times (v_{ej}/10^{3.5} \text{ km s}^{-1})^{1/3} \qquad (17)$$

According to Eqn. (16), a cosmic-ray reaches a momentum equal to 50% of p_{∞} at a time $t = 29\, t_1 \approx 10^5$ yrs, for the nominal parameters used to normalize the above expressions. However the asymptotic momentum attainable, p_{∞}, will be considerably less than the observed value of 10^{14} - 10^{15} eV/c unless $\delta B / B_0 \geq 1$ and some of the physical parameters in Eqn. (17) differ substantially from the nominal values to which they have been normalized here.

The parameter $\delta B/B_0$ is of course a function of the actual physical conditions near the supernova remnant shock, and must be determined self-consistently as a function of the externally given environment. We can use our simulation results to relate $\delta B/B_0$ to the upstream *flux* of cosmic-rays, J_{cr}, defined dimensionlessly as

$$J_{cr} = (n_{cr}\, v_{cr}) / (n_{ism}\, v_A) . \qquad (18)$$

Figure 8 shows the dependence of $\delta B/B_0$ on J_{cr} in our simulations. The result is a strikingly simple power-law,

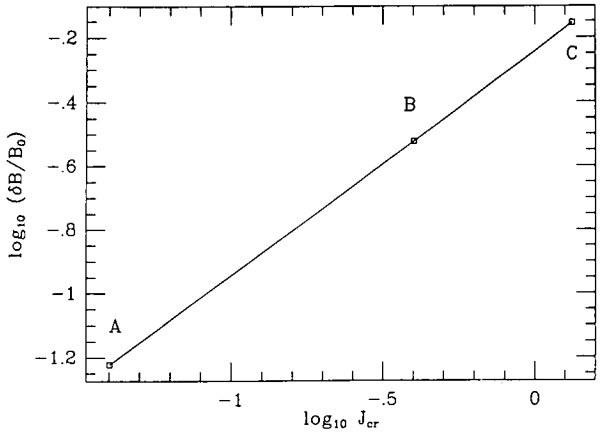

Figure 8: Scaling relation betwen root-mean-square amplitude of magnetic field perturbations $\delta B/B_0$, and normalized cosmic-ray flux J_{cr} , from our simulations.

$$\delta B/B_0 = 0.57\, J_{cr}^{0.7} . \qquad (19)$$

If we substitute this relation into Eqn. (8) for the cosmic-ray diffusion coefficient, we find that

$$D = (r_L\, v\, /3\,)\,(59\, J_{cr}^{-2.1}) \qquad (20)$$

for $1.3 > J_{cr} > 0.6$. If one extrapolates this relation to somewhat larger fluxes, we obtain the result that $D < r_L\, v\, /3$ for $J_{cr} > 7$. Previous authors (e.g. Refs. 2 and 3 and references therein) have suggested that $D = r_L\, v\, /3$ is a minimum value for the cosmic-ray diffusion coefficient. However the mean free path can be smaller than the Larmor radius in the background field, r_L, because the fluctuating fields can be larger in magnitude than the background field when $J_{cr} > 3$, and because transitory strong trapping in the turbulent magnetic fields can reduce the mean free path while still allowing the particles to diffuse.

We can substitute Eqn. (19) into expression (17) for p_∞ , and derive the asymptotic maximum cosmic-ray energy as a function of J_{cr} . For simplicity we take $Z/A = 1$, since the mechanism must work for protons. Then in the range $0.6 \le J_{cr} \le 1.3$, we have

$$p_\infty \approx (1.4 \times 10^{12}\ \mathrm{eV/c}) \times J_{cr}^{2.1 \pm 0.4}\, (B_0/\ 10^{-6}\ \mathrm{gauss}) \times (E_{SN}/10^{51}\ \mathrm{ergs})^{1/3}\, (n_{ism}/10^{-2}\ \mathrm{cm^{-3}})^{-1/3} \times (v_{ej}/10^{3.5}\ \mathrm{km\ s^{-1}})^{1/3} ; \qquad (21)$$

while for $0.04 \le J_{cr} \le 0.6$, we have

$$p_\infty \approx (0.45 \times 10^{12}\ \mathrm{eV/c}) \times J_{cr}^{0.28}\, (B_0/\ 10^{-6}\ \mathrm{gauss}) \times (E_{SN}/10^{51}\ \mathrm{ergs})^{1/3}\, (n_{ism}/10^{-2}\ \mathrm{cm^{-3}})^{-1/3} \times (v_{ej}/10^{3.5}\ \mathrm{km\ s^{-1}})^{1/3}. \qquad (22)$$

The numerical value of the asymptotic cosmic-ray momentum p_∞ predicted by Eqns. (21) and (22) depends on the cosmic-ray flux J_{cr} , and weakly on the physical characteristics of the supernova remnant and its surroundings. First consider the variation of p_∞ with J_{cr} , and assume that the other physical parameters take on the normalization values indicated in Eqns. (21) and (22). Then over the range we have simulated, $0.04 \le J_{cr} \le 1.3$, the factors containing J_{cr} in Eqns. (21) and (22) lead to a relatively narrow variation of p_∞ : $0.2 \times 10^{12} \le p_\infty \le 2.4 \times 10^{12}$ eV/c . The observed maximum cosmic-ray momentum is considerably larger than this range. In order to produce realistically large cosmic-ray momenta by varying J_{cr} alone, one would have to extrapolate our results to the regime $J_{cr} >> 1$, where $\delta B/B_0 > 1$.

Because of the weak dependence of p_∞ in (21) and (22) on the parameters of the supernova explosion and the interstellar medium, $J_{cr} \ge 8$ is the only way consistent with the normal energetics and velocities of supernovae to raise p_∞ to its observed value $\approx 10^{15}$ eV. Under such circumstances the cosmic-ray pressure can alter both the shock structure and the value of u_1 used in Eqn. (14). For the p^{-4} momentum spectrum expected in the simplest form of shock acceleration, with the minimum momentum p_{min} comparable to the thermal momentum of the shocked interstellar medium, $p_{cr} < \rho v^2$ implies

$$J_{cr} < 0.9\, (100\ \mathrm{keV}/E_{min})^{1/2}\, (v_{ej}/10^{3.5}\ \mathrm{km\ s^{-1}})^3 \times (n_{ism}/10^{-2}\ \mathrm{cm^{-3}})^{1/2}\, (B_0/10^{-6}\ \mathrm{gauss})^{-1/2} \times \{\, 33/[\,1 + 2\ln(p_{max}/mc)\,]\,\}\, (t_1/t)^{6/5} \qquad (23)$$

Here, $E_{min} = p_{min}^2/2m$ is the kinetic energy corresponding to the lower cutoff of the momentum distribution. The fact that x-ray emission from galactic supernova remnants is in rough accord with the predictions of supernova remnant models having $p_{cr} < \rho v^2$ upstream (Ref. 3) therefore suggests that $J_{cr} >> 1$ is unlikely in Type II supernovae. However, the higher velocity Type I supernova remnants ($v_{ej} \approx 10^4$ km s^{-1}) have a much larger kinetic energy flux upstream from the shock for the same age relative to t_1, and thus may be able to have high cosmic ray flux while still satisfying $p_{cr} < \rho v^2$; J_{cr} as large as 25 is allowed by Eqn. (23), corresponding to $\delta B/B_0$ up to 5.5 in the cosmic ray foreshock. From Eqn. (21), we find $p_\infty \approx 10^{15}$ eV/c if $J_{cr} \approx 19$, corresponding to very strong turbulence $\delta B/B_0 \approx 5$, a value marginally within the dynamical constraints. Thus, on dynamical grounds, Type I supernova remnants may be the most favorable site for shock acceleration. One should note that observations of the rate of supernova occurence, lifetime of cosmic rays in the galaxy inferred from the abundances of heavy nuclei in the cosmic rays, and the number density of cosmic rays, can be used to suggest that $J_{cr} < 1$ even in Type I remnants during the acceleration phase (Zachary, Max and Arons, in preparation). This conclusion militates against the formation of large $\delta B/B_0$ even in Type I supernova remnants. However, recent work (e.g., Ref. 9) has suggested that the protons may have undergone a different history in the galaxy from that experienced by the heavy nuclei. If the proton lifetime is a factor of ten shorter than that of the heavy nuclei, our results suggest that shock acceleration in Type I remnants remains a viable candidate for the origin of cosmic rays.

In summary, extrapolation of our simulation results to high-energy cosmic rays implies an upper limit of about

10^{12} eV for the maximum energy attainable in shock-acceleration at Type II supernova remnant shocks. This is several orders of magnitude less than the observed maximum energy of the power-law source distribution of cosmic rays. On the other hand, the expansion of Type I supernovae into the low density phase of the interstellar medium may be able to accelerate cosmic rays to energies comparable with the observed upper cutoff of the smooth power-law distribution, if the very large field amplitudes implied by our simulations are applicable to the long wavelength magnetic fluctuations with which the highest energy particles interact.

This research was supported by the US Department of Energy, under contract number W-7405-ENG-48 to the Lawrence Livermore National Laboratory; by the US National Science Foundation, under grant number AST-8615816 to the University of California; by the Institute of Geophysics and Planetary Physics at LLNL, under grant number 89-11; by the NASA Theoretical Astrophysics Program, under grant number NAGW-1301 to the California Institute of Technology and the University of California; and by NSF grant number AST-8503093, awarded to the University of Chicago.

5. FOOTNOTES AND REFERENCES

* Institute of Geophysics and Planetary Physics, Plasma Physics Research Institute, Physics Department, and A Division.

+ Departments of Astronomy and of Physics.

1 A. R. Bell, *M.N.R.A.S.* 182, 147 and 443 (1978); G.F. Krymsky, *Sov. Phys. Dokl.* 23, 327 (1977); I. Axford, E. Leer, and G. Skadron, *Proc. 15th International Ray Conference, Plovdiv*, vol. 11 (Central Research Institute for Physics, Budapest), p. 132 (1977); R.D. Blandford and J.P. Ostriker, *Astrophys. J. Lett.* 221, L229 (1978).

2 P.O. Lagage and C.J. Cesarsky, *Astron. Astrophys.* 125, 249 (1983).

3 R. Blandford and D. Eichler, *Phys. Reports* 154, 1 (1987).

4 C.F. Kennel, F.V. Coroniti, F.L. Scott, W.A. Livesy, C.T. Russell, E.J. Smith, K.P. Wenzel, and M. Scholer, *J. Geophys. Res.* 91, 11917 (1986).

5 A.L. Zachary and B.I. Cohen, *J. Comput. Phys.* 66, 469 (1986).

6 A.L. Zachary, *Resonant Alfven Wave Instabilities Driven by Streaming Fast Particles*, Ph.D. Dissertation, Astronomy Department, University of California, Berkeley (1987). University of California Report no. UCRL-53793, Lawrence Livermore National Laboratory.

7 C.E. Max, A.L. Zachary and J. Arons, Interstellar Electron Density Fluctuations Due to Cosmic-Ray Acceleration at Supernova Remnant Shock Waves, *Radio Wave Scattering in the Interstellar Medium* (Amer. Inst. Physics, NY, 1988), edited by J. Cordes.

8 J. R. Jokipii, *Rev. Geophys. Space Phys.* 9, 27 (1971).

9 C.J. Cesarsky, 1988, in *Proc. Joint Varenna-Abastumani Workshop on Plasma Astrophysics*, these proceedings